

## Imaging of Features on Surfaces by Condensation Figures

Gabriel P. López, Hans A. Biebuyck, C. Daniel Frisbie,  
George M. Whitesides\*

Condensation of a vapor to a liquid on a cold surface that is not wet completely by this liquid leads to the formation of an array of droplets. If the surface is heterogeneous in its physical properties (especially its interfacial free energy), the patterns of these arrays reflect this heterogeneity. The distribution of droplets of water (condensation figures or CFs) observed by optical microscopy on a surface can be correlated with the molecular structure of that surface. The substrates used to investigate the formation and morphology of the CFs were patterned, self-assembled monolayers of different alkanethiolates on gold and of alkyl siloxanes on glass. Analysis of CFs is a valuable nondestructive technique for characterizing heterogeneities in surfaces.

Condensation figures (CFs)—historically called “breath figures” because they appear on cool surfaces exposed to warm, humid air (from exhaled breath) (1)—form images of regions with different wettabilities in self-assembled monolayers (SAMs). The formation of breath figures and their use as a method for detecting contamination on homogeneous surfaces was described by Lord Rayleigh and later by Méricoux (1). In general, CFs are an example of phenomena that have a basis in heterogeneous nucleation: Technologically important examples include (i) the growth of thin films of metals and semiconductors during evaporative plating and chemical vapor deposition and (ii) the condensation of liquids in heat transfer operations. As an example of heterogeneous nucleation and condensation, CFs of water are conveniently studied at near room temperature and hence have been investigated experimentally (2, 3) and theoretically (3, 4).

At a particular stage in the development of a CF, differences in the size and distribution of the droplets reflect properties of the surface on which they form. We used optical microscopy of CFs to image patterns in two types of patterned SAMs: SAMs formed from two or more different,  $\omega$ -substituted alkanethiolates on gold (5) and SAMs formed by the silanization of glass with two or more functionalized alkyltrichlorosilanes (6, 7). These studies indicate that CFs on SAMs will be valuable as a method of surface analysis and as a tool in understanding nucleation and growth of condensed phases at interfaces. The ease with which SAMs can be used to control surface wettability and the ability to use them to generate patterns of areas that differ in their wettability make SAMs particularly convenient substrates with which

to develop these analytical methods and with which to test hypotheses regarding the formation and growth of CFs.

Figure 1 shows an optical micrograph of a CF on a sample (8) in which patterns have been formed with SAMs derived from  $\text{HS}(\text{CH}_2)_{15}\text{CH}_3$ ,  $\text{HS}(\text{CH}_2)_{15}\text{CH}_2\text{OH}$ , and  $[\text{S}(\text{CH}_2)_{16}\text{CN}]_2$  (9). These patterns were not detectable by optical microscopy before the CF formed (see Fig. 2C, for example). It is clear from Fig. 1 that CFs form useful images of surfaces that differ primarily in their interfacial free energies and that they can produce images with good contrast. Contrast between regions of different alkanethiolates is a consequence of differences in the distributions of water across these regions. This distribution at a particular time is characterized by differences in droplet size, density, polydispersity, and structure factor (2).

Earlier studies of the mechanisms of drop growth and coalescence on homogeneous surfaces bear directly on the use of CFs as a quantitative technique for imaging heterogeneous surfaces (2–4). Knobler, Meakin, and other investigators have identified several distinct phases that occur in the formation of a CF on a homogeneous surface (2–4). The earliest stage involves the uniform coverage of the surface by the nucleation of small droplets that grow with few coalescences. Subsequent stages include a regime in which the droplet distribution remains, with growth and coalescence, similar in time and exhibits a well-defined structure factor. This stage is followed by a regime in which nucleation of new droplets occurs between older and larger drops. Typically, the stage of CF evolution in which droplet coalescence is negligible gives images with the highest sensitivity and resolution.

To correlate the appearance of the CF to chemical functionality on the surface, we imaged a single line of a SAM derived from hexadecanethiol- $d_{33}$ ,  $[\text{HS}(\text{CD}_2)_{15}\text{CD}_3]$  embedded in a SAM derived from mercapto-

hexadecanoic acid  $[\text{HS}(\text{CH}_2)_{15}\text{CO}_2\text{H}]$  (10). We compared images (Fig. 2) of CFs obtained by optical microscopy to images of the same surface feature obtained by secondary ion mass spectrometry (SIMS) (11) and scanning electron microscopy (SEM) (12). All three techniques yielded images with similar lateral resolution. For CFs, sensitivity to surface features and image resolution depends on several factors, including the stage of growth of the CF, the rate of condensation, and the type of surface.

We used a patterned SAM consisting of a rectilinear grid (line width  $\sim 10\ \mu\text{m}$  and line spacing  $\sim 10\ \mu\text{m}$ ) of hydrophobic lines (contact angle of water  $\sim 120^\circ$ ) bounding hydrophilic squares (contact angle of water  $\sim 30^\circ$ ) to control the pattern of coalescence explicitly (13). We expected the grid to impose a pattern on the position of the drops. Figure 3 shows the evolution of a CF of water on this patterned surface.

In the top micrograph in Fig. 3, the condensation of water has progressed only to the point of forming one drop on each hydrophilic region; there has been no drop coalescence. At this stage, the volume of each drop is approximately  $10^{-7}\ \mu\text{l}$  ( $10^2\ \mu\text{m}^3$ , roughly the volume of an erythro-

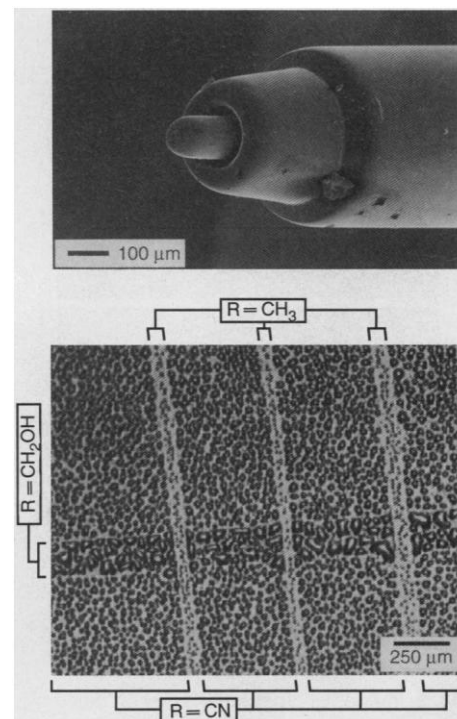


**Fig. 1.** (Top) Scanning electron micrograph of a micropen tip. Lines of SAMs derived from  $\text{HS}(\text{CH}_2)_{15}\text{CH}_3$  were written with the use of this pen. A micropipette was used to write a SAM derived from  $\text{HS}(\text{CH}_2)_{15}\text{CH}_2\text{OH}$ . The background, derived from  $[\text{S}(\text{CH}_2)_{16}\text{CN}]_2$ , was formed in a subsequent step. (Bottom) Optical micrograph of a CF of the pattern of SAMs composed of the alkanethiolates  $\text{R}(\text{CH}_2)_{15}\text{S}^-$  ( $\text{R} = \text{CH}_3, \text{CO}_2\text{H}, \text{CN}$ ).

Department of Chemistry, Harvard University, Cambridge, MA 02138.

\*To whom correspondence should be addressed.

cyte); we believe that this type of array will be useful in analytical methods in which these small, isolated volumes of liquids serve as microreactors. Moreover, CFs can be sensitive analytical tools for the detection of defects on surfaces that are either patterned (as in the present example) or meant to be uniform. Because a small defect in the area of the hydrophobic grid can result in the nucleation of a stable droplet of water, the presence of drops (arrow in Fig. 3) outside the ordered array of condensate suggests a defect in the desired pattern. Although the detection limit of CFs as a tool for inspection remains to be determined, Fig. 3 suggests that nucleation of a

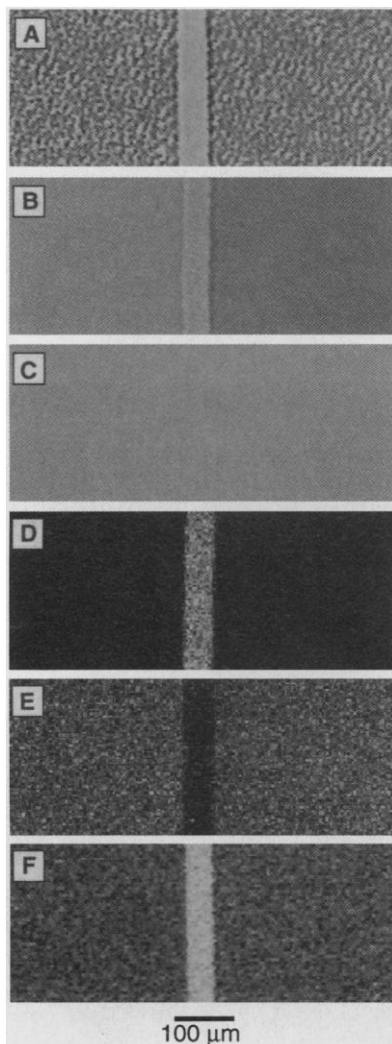


**Fig. 2.** Images of a patterned SAM obtained by different techniques. The surface consists of a line of a SAM obtained by the adsorption of  $\text{HS}(\text{CD}_2)_{15}\text{CD}_3$  within a SAM obtained from  $\text{HS}(\text{CH}_2)_{15}\text{CO}_2\text{H}$ . (A) Optical micrograph of a CF formed from water on the patterned SAM; (B) optical micrograph of the CF shown in (A) after further condensation; (C) optical micrograph of the sample without formation of a CF; (D) SIMS ion map ( $m/z = 50$ ); (E) SIMS ion map ( $m/z = 55$ ); (F) scanning electron micrograph of the patterned SAM.

drop on a defect, followed by its growth through controlled condensation, will make possible the detection of submicrometer-sized defects.

Figure 3 illustrates the potential of an array patterned in its hydrophilicity as a model system with which to study evolution of CFs with time. Typically, the round ( $\sim 10 \mu\text{m}$  in diameter) drops first combine with other round drops to form elongated drops, which are constrained in their shape by the underlying wettability of the hydrophilic interstitial spaces. Because capillary effects tend to drive the drops toward their equilibrium shape (a spherical cap that has an equilibrium contact angle with the hydrophobic surface), the growth of the drops, by condensation to them, tends to make them rounder (that is, the minor axis of the ellipsoid grows faster than the major axis). With further condensation, the remaining round and elongated drops may coalesce to form triangles, or two parallel elongated drops may coalesce to form a square. Hence, in this rectangular array, elongated drops do not coalesce end to end and form lines; instead, triangles and squares form with increased condensation.

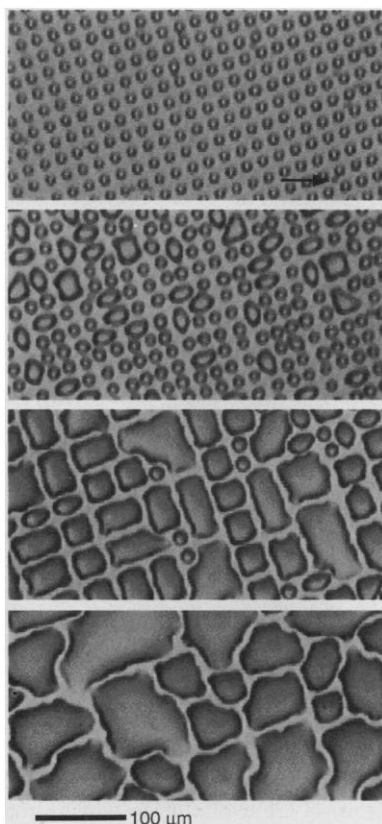


**Fig. 3.** Evolution of a CF of water with time on a patterned surface (top to bottom). The surface consists of a grid of perpendicular lines of a hydrophobic SAM derived from  $\text{Cl}_3\text{Si}(\text{CH}_2)_2(\text{CF}_2)_5\text{CF}_3$  with square interstices of SAMs derived from  $\text{Cl}_3\text{Si}(\text{CH}_2)_9\text{CH}=\text{CH}_2$  that have been rendered hydrophilic by oxidation.

Examination of CFs formed on regular grids should provide a wealth of information about the rules regulating their evolution with further condensation.

For surfaces having patterns with features of dimensions  $\geq \sim 10 \mu\text{m}$ , CFs offer a method of imaging that is simple, nondestructive, and inexpensive. CFs are sensitive to parameters such as interfacial free energy, chemical reactivity, and functional group character that may not be detected by other techniques (14). Formation of CFs can be rapid ( $\sim 1 \text{ s}$ ) and, in principle, reversible; CFs can be generated and "erased" (by evaporation) repeatedly and used to follow changes in a surface. A wide variety of vapors with different characteristics can be used in forming CFs.

Because organic surfaces (including SAMs) are damaged by exposure to particle beams [ions (11), electrons (15), and atoms (16)], truly nondestructive imaging is not possible if one uses spectroscopic methods such as SIMs, scanning Auger microscopy, SEM, x-ray photoelectron spectroscopy (15), or silver decoration (17). CFs provide a method of surface imaging with minimal potential for damaging most surfaces. We have used CFs to image nondestructively the surfaces of several types of patterned surfaces (for example, ceramics and polystyrene that has been selectively damaged by an electron beam) (18).

The ultimate spatial resolution possible in imaging with CFs remains to be defined, as does the correspondence of the size, shape, and distribution of droplets to specific physical, chemical, and morphological features of the surface, and to the method of CF formation. In these pursuits, as in the present study, the synthetic versatility of patterned SAMs will be invaluable (5).

## REFERENCES AND NOTES

1. Lord Rayleigh, *Nature* **86**, 416 (1911); J. Aitken, *ibid.*, p. 516; Lord Rayleigh, *ibid.* **90**, 436 (1912); R. Mérieux, *Rev. Opt.* **9**, 281 (1937).
2. C. M. Knobler, *Physica A* **140**, 198 (1986); D. Beysens and C. M. Knobler, *Phys. Rev. Lett.* **57**, 1433 (1986); F. Perrot and D. Beysens, *Rev. Sci. Instrum.* **58**, 183 (1987); B. J. Briscoe and K. P. Galvin, *Colloids Surf.* **56**, 263 (1991).
3. D. Fritter, C. M. Knobler, D. Beysens, *Phys. Rev. A* **43**, 2858 (1991); A. Steyer, P. Guenoun, D. Beysens, C. M. Knobler, *ibid.* **44**, 8271 (1991).
4. J. L. Viowy, D. Beysens, C. M. Knobler, *ibid.* **37**, 4965 (1988); A. Steyer, P. Guenoun, D. Beysens, D. Fritter, C. M. Knobler, *Europhys. Lett.* **12**, 211 (1990); P. Meakin and F. Family, *J. Phys. A Math. Gen.* **22**, L225 (1989); F. Family and P. Meakin, *Phys. Rev. A* **40**, 3836 (1989); B. J. Briscoe and K. P. Galvin, *J. Phys. D* **23**, 422 (1990); B. Derrida, C. Godrèche, I. Yekutieli, *Europhys. Lett.* **12**, 385 (1990).
5. C. D. Bain and G. M. Whitesides, *J. Am. Chem. Soc.* **111**, 7164 (1989); G. M. Whitesides and P. E. Laibinis, *Langmuir* **6**, 87 (1990).
6. J. Sagiv, *J. Am. Chem. Soc.* **102**, 92 (1980).
7. S. R. Wasserman, Y.-T. Tao, G. M. Whitesides, *Langmuir* **5**, 1074 (1989).
8. The sample containing the patterned SAM was placed on a silicon stage in a chamber fed by a

near saturated stream of water vapor in argon. CFs formed by condensation of water as the stage was cooled to  $\sim 0^\circ\text{C}$ .

9. To form the patterned SAMs of alkanethiolates on a gold substrate, a micropipen was used first to write lines of a hydrophobic SAM from neat hexadecanethiol [ $\text{HS}(\text{CH}_2)_{15}\text{CH}_3$ ], and then a micropipette was used to form a hydrophilic SAM from mercaptohexadecanoic acid [ $\text{HS}(\text{CH}_2)_{15}\text{CO}_2\text{H}$ ]; see A. Kumar, H. A. Biebuyck, N. L. Abbott, G. M. Whitesides, *J. Am. Chem. Soc.*, in press. The SAM derived from  $\text{HS}(\text{CH}_2)_{15}\text{CH}_3$  was written in air. To write the hydrophilic line, a micropipette was loaded with a concentrated solution of  $\text{HS}(\text{CH}_2)_{15}\text{CO}_2\text{H}$  in hexadecane. The tip of the micropipette and the gold surface were placed under water. The water prevented spreading and trailing of the thiol solution during writing. During writing, the tips of the pen and micropipette did not touch the surface of the gold; only liquid containing the alkanethiol contacted the gold. There was therefore no mechanical marking of the gold surface. After formation of the desired patterns, the gold was exposed to a 1 mM solution of  $[\text{S}(\text{CH}_2)_{16}\text{CN}]_2$  for 1 min. The disulfide  $[\text{S}(\text{CH}_2)_{16}\text{CN}]_2$ , rather than the corresponding thiol, was used to complete the SAM of alkanethiolates because the rate of exchange of the preformed, alkanethiolate SAMs (lines in Fig. 1) is slower with disulfide than with thiol (H. A. Biebuyck and G. M. Whitesides, unpublished results).
10. The line was obtained by writing of  $\text{HS}(\text{CD}_2)_{15}\text{CD}_3$  with a micropipen in air. A 1 mM  $\text{HS}(\text{CH}_2)_{15}\text{CO}_2\text{H}$  solution in ethanol was reactively spread on either side of the hydrophobic line and allowed to react for 1 min to derivatize the remainder of the gold surface.
11. Typical SIMS analysis conditions were as follows. A primary ion beam of 16 keV  $\text{Ga}^+$  ions (50 pA) was used. The maps obtained are a 256 pixel by 256 pixel image with a dwell time of 200  $\mu\text{s}$  per pixel. We believe the peak at a mass-to-charge ratio  $m/z = 50$  to be primarily due to  $\text{C}_3\text{D}_7^+$ ; that at  $m/z = 55$  is attributable to  $\text{C}_3\text{H}_5\text{O}^+$  and  $\text{C}_4\text{H}_7^+$ . For further details see C. D. Frisbie, J. R. Martin, R. R. Duff, M. S. Wrighton, *J. Am. Chem. Soc.* 114, 7142 (1992).
12. G. P. López, H. A. Biebuyck, G. M. Whitesides, unpublished results; E. W. Wollman, C. D. Frisbie, M. S. Wrighton, unpublished results.
13. Pyrex glass wafers (Mooney Precision Glass, Huntington, WV) were cleaned in piranha solution [see (5)], rinsed with deionized water, and dehydrated under  $\text{N}_2$  at  $200^\circ\text{C}$  for 8 hours. A 1- $\mu\text{m}$  layer of positive photoresist (KTI 820, 20 centistokes, Union Carbide) was spin coated onto the glass wafers. The coated wafers were baked at  $90^\circ\text{C}$  for 30 min and then exposed to ultraviolet light in an infrared aligner (Carl Suss, Munich, Germany) through a chrome mask containing the desired pattern. We removed the exposed photoresist by treating the photoresist with KTI-934 (1:1) developer (Union Carbide). The remaining photoresist was used to restrict the deposition of vaporized (tridecafluoro-1,1,2,2-tetrahydrooctyl)-1-trichlorosilane [ $\text{Cl}_3\text{Si}(\text{CH}_2)_2(\text{CF}_2)_5\text{CF}_3$ ] to certain regions of the surface of the glass. Photopatterned glass wafers were placed in a vacuum desiccator (in a dry box) together with an open vial containing 30  $\mu\text{l}$  of  $\text{Cl}_3\text{Si}(\text{CH}_2)_2(\text{CF}_2)_5\text{CF}_3$  for 20 min. The vial and the remaining liquid were then removed from the desiccator, which was evacuated with continuous pumping for 1 hour. The wafers were then removed from the desiccator, and the photoresist was lifted off by sonication in ethanol. After drying, the newly exposed glass surfaces were derivatized (as above) by exposure to 10-undecenyl-1-trichlorosilane [ $\text{Cl}_3\text{Si}(\text{CH}_2)_9\text{CH}=\text{CH}_2$ ] vapors. This procedure resulted in a patterned surface of fluorinated and vinyl-terminated monolayers. We then selectively rendered the vinyl-terminated monolayers hydrophilic by placing the wafers in an aqueous oxidant solution (1.0 mM  $\text{KMnO}_4$ ; 40 mM  $\text{NaIO}_4$ ; 4 mM  $\text{K}_2\text{CO}_3$ ; pH 7.5) for 15 min. The wafer was removed from this solution and rinsed in 10 ml of each of 1 M

- NaHSO<sub>3</sub>, water, 0.1 N HCl, and ethanol [see (7)].
14. L. Vroman, *Thromb. Diath. Haemorrh.* 10, 455 (1963); H. Elwing, *FEBS Lett.* 111, 365 (1980).
15. P. A. Laibinis, R. L. Graham, H. A. Biebuyck, G. M. Whitesides, *Science* 254, 981 (1991).
16. M. J. Tarlov, *Langmuir* 8, 80 (1992).
17. C. Bubeck, *Thin Solid Films* 178, 483 (1989).
18. H. A. Biebuyck and G. M. Whitesides, unpublished results.
19. We thank R. Singhvi for providing the photopatterned poly(methyl methacrylate)-glass samples for silanization. This research was supported in

part by the Office of Naval Research and the Defense Advanced Research Projects Agency. We obtained SIMS ion maps using instrument facilities purchased under the Defense Advanced Research Projects Agency-University Research Initiative program. G.P.L. thanks the Ford Foundation for a postdoctoral fellowship and the National Institutes of Health for supplementary funds provided under the initiative to increase the participation of underrepresented minorities in research.

9 November 1992; accepted 17 February 1993

## Condensed-Matter Energetics from Diatomic Molecular Spectra

In Ho Kim, Raymond Jeanloz,\* Kyu Soo Jhung

Analyses of molecular spectra and compression data from crystals show that a single function successfully describes the dependence on interatomic separation of both the potential energy of diatomic molecules and the cohesive binding energy of condensed matter. The empirical finding that one function describes interatomic energies for such diverse forms of matter and over a wide range of conditions can be used to extend condensed-matter equations of state but warrants further theoretical study.

**P**rediction of the energetics of many-body systems from a detailed model of two-body interactions among the constituent particles has long been a matter of interest. Thus, considerable effort has gone into the derivation of reliable expressions for the potential-energy functions of two-atom systems (1, 2), and substantial progress has been made toward the discovery of a universal description of these diatomic potentials (3–8). Ideally, such a universal description reduces to a single potential-energy function that is valid for all diatomic systems. Similarly, universal correlations have been uncovered in recent work on the energetics of many-atom systems. For example, one equation of state appears to describe interparticle forces ranging from adhesion at large separations to nuclear compression at short ranges (5, 9). Here we develop in more detail, and using a different approach, a surprisingly reliable description of binding energy that spans the range from diatomic molecules to condensed matter (10).

The binding energy of a diatomic molecule can be expressed as a modified Dunham expansion of the reduced energy  $f = E(R)/E_e$ , which has the form

$$f(z_1) = z_1^2 \left( 1 + \sum_{n=1}^{\infty} \beta_n z_1^n \right) - 1 \quad (1)$$

in terms of the linear scaled distance used by many investigators (5–11)

$$z_1 = \sqrt{\Delta} (R/R_e - 1) \quad (2)$$

Here  $R_e$  and  $E_e$  are the equilibrium values of the interparticle distance  $R$  and potential energy  $E(R)$  of the molecule. The  $\beta_n$  are related to the Dunham coefficients,  $a_n$ , by the relation  $\beta_n = a_n/\Delta^{n/2}$ , where  $\Delta$  is the Sutherland parameter, a material-dependent scale factor corresponding to the equilibrium force constant of a harmonic oscillator (11, 12). If all  $\beta_n$  equal zero, the reduced potential  $f$  is that of a harmonic oscillator. Alternatively, if we assign an equal amount of anharmonicity to all diatomic molecules, then each  $\beta_n$  is independent of the molecule involved (13).

Diatomic molecules exhibit a wide range of anharmonicity, however, and linear scaling of interatomic distances as given by Eq. 2 is inadequate because it implies  $\beta_1$  and  $\beta_2$  are constant for all systems (Fig. 1A). Instead, a more flexible nonlinear scaling, including molecule-dependent excess parameters, seems to be required. This is facilitated by the observation that the spectroscopically determined anharmonicity parameters  $\beta_1$  and  $\beta_2$  are correlated (Fig. 1A'). The strong correlation is not limited to two dimensions but still holds in multidimensional  $\beta$ -space, at least up to four  $\beta$ -dimensions (14). Therefore, we can regard this correlation as an expression that can generate  $\beta_{n+1}$  from  $\beta_n$ , a recursion relation for

I. H. Kim, Department of Geology and Geophysics, University of California, Berkeley, CA 94720, and Agency for Defense Development, Yuseong Post Office Box 35, Taejeon 305-600, South Korea.  
R. Jeanloz, Department of Geology and Geophysics, University of California, Berkeley, CA 94720.  
K. S. Jhung, Agency for Defense Development, Yuseong Post Office Box 35, Taejeon 305-600, South Korea.

\*To whom correspondence should be addressed.